

Characteristic Method Applied to Blast Waves in a Dusty Gas

Fumio Higashino *

Stoßwellenlabor der Rheinisch-Westfälischen Technischen Hochschule Aachen

Z. Naturforsch. **38 a**, 399–406 (1983); received November 6, 1982

The unsteady propagation of shock waves in a dusty gas is investigated theoretically. The characteristic equations are obtained without neglecting the effect of the partial pressure of the particles. Numerical computations were carried out by Hartree's technique. As examples, the flow in a shock tube and in a blast wave is examined by applying a generalized piston problem. The results show that the existence of suspended particles may cause a rapid decay of the shock strength and that the flow field is divided into several regimes which are characterized by the shock position and the relaxation times.

Introduction

In spite of many studies on blast waves in a dust-free gas, only a few analyses about heterogeneous systems [1, 2] exist. Gerber and Bartos [2] have studied the motion of individual particles in the mixture. In this case the problem reduces to the analysis of the trajectories of single particles while the interactions of the particles with other particles and the gas flow are neglected. In general, however, the momentum and energy exchange between the gas and the particles should be taken into account except for a flow with temperature and velocity equilibrium. We have already analysed the problem of a strong blast wave under the assumption of temperature and velocity equilibrium and got similarity solutions [1, 2].

In the present work, nonuniform propagation of shock waves in a dusty gas is investigated in order to clarify the effects of the interparticle and particle-gas interactions during the relaxation process. The characteristics method of Hartree was applied, since it is difficult to get a similarity solution. Rudinger and Chang [3] have already investigated the nonsteady two-phase flow in a shock tube by applying the standard method of characteristics. They suggested that the partial pressure of the particles should be neglected in order to get compatibility equations free from partial derivatives when utilizing the characteristics method. They also neglected the effect of volume fraction of the particles. However, we noticed that it is not necessary to ne-

glect the volume fraction when the generalized method of characteristics in matrix form is applied to the system of partial differential equations for two phase flow. It should be emphasized that the propagation of small disturbances is slower in the mixture than in the dust-free gas.

To treat the piston problem in general and to remove the difficulty concerning the singularity at the center of the explosion, the motion of the contact surface was assumed to decay exponentially with time. In this way the relaxation processes of plane shock waves corresponding to shock tube flow as well as blast waves were investigated.

Basic Equations

We consider the motion of a continuous medium containing solid or liquid spherical particles. To analyze such a two phase medium one is compelled to make assumptions regarding the dust particles and their interaction with the gas flow. In the present study we employed the same assumptions as in the previous work [1] except for the condition of temperature and velocity equilibrium between the gas and the particles. The motion of the two phase medium is governed by the conservation laws of mass, momentum and energy for the mixture and particles. They may be expressed in a vectorized form as

$$A Z_t + B Z_r + C = 0, \quad (1)$$

$$A = \begin{pmatrix} 0 & 0 & 1 & 0 & 0 & 0 \\ 0 & 0 & 0 & 0 & 1 & 0 \\ \varrho_g & 0 & 0 & \varrho_p & 0 & 0 \\ 0 & \alpha_1 & \alpha_2 & \alpha_3 & 0 & \alpha_4 \\ 0 & 0 & 0 & \varrho_p & 0 & 0 \\ 0 & 0 & 0 & 0 & 0 & c \varrho_p \end{pmatrix}, \quad Z = \begin{pmatrix} U_g \\ p \\ \varrho_g \\ U_p \\ \varrho_p \\ T_p \end{pmatrix}, \quad (2)$$

* On Leave from Department of Mechanical Engineering, Tokyo-Noko University, Tokyo 184 Japan.

Reprint requests to Prof. F. Higashino, Department of Mechanical Engineering, Tokyo University of Agriculture and Technology, Koganei-shi, Tokyo 184/Japan.

0340-4811 / 83 / 0400-0399 \$ 01.3 0/0. – Please order a reprint rather than making your own copy.



Dieses Werk wurde im Jahr 2013 vom Verlag Zeitschrift für Naturforschung in Zusammenarbeit mit der Max-Planck-Gesellschaft zur Förderung der Wissenschaften e.V. digitalisiert und unter folgender Lizenz veröffentlicht: Creative Commons Namensnennung-Keine Bearbeitung 3.0 Deutschland Lizenz.

Zum 01.01.2015 ist eine Anpassung der Lizenzbedingungen (Entfall der Creative Commons Lizenzbedingung „Keine Bearbeitung“) beabsichtigt, um eine Nachnutzung auch im Rahmen zukünftiger wissenschaftlicher Nutzungsformen zu ermöglichen.

This work has been digitalized and published in 2013 by Verlag Zeitschrift für Naturforschung in cooperation with the Max Planck Society for the Advancement of Science under a Creative Commons Attribution-NoDerivs 3.0 Germany License.

On 01.01.2015 it is planned to change the License Conditions (the removal of the Creative Commons License condition "no derivative works"). This is to allow reuse in the area of future scientific usage.

$$B = \begin{pmatrix} \rho_g & 0 & U_g & 0 & 0 & 0 \\ 0 & 0 & 0 & \rho_p & U_p & 0 \\ \rho_g U_g & 1 & 0 & \rho_p U_p & 0 & 0 \\ \beta_1 & \beta_2 & \alpha_2 U_g & \beta_3 & 0 & \alpha_4 \\ 0 & \varepsilon & 0 & \rho_p U_p & 0 & 0 \\ 0 & 0 & 0 & 0 & 0 & c \rho_p U_p \end{pmatrix},$$

and

$$C = \begin{pmatrix} \frac{j}{r} \rho_g U_g \\ \frac{j}{r} \rho_p U_p \\ 0 \\ \frac{j}{r} U_m \varepsilon p \\ -F \\ -Q \end{pmatrix}, \quad (3)$$

where

$$\begin{aligned} \alpha_1 &= 1 - \varepsilon, \quad \alpha_2 = -(\gamma - \varepsilon) p / \rho_g, \quad \alpha_3 = \rho_p U_m \\ \alpha_4 &= (\gamma - 1) c \rho_p, \quad U_m = (\gamma - 1) (U_p - U_g), \\ \beta_1 &= -(\gamma - 1) \varepsilon p, \quad \beta_2 = U_g + \varepsilon (U_m - U_g), \\ \beta_3 &= \rho_p U_p U_m + (\gamma - 1) \varepsilon p. \end{aligned}$$

The subscripts t and r of Z represent the partial derivatives with respect to time t and spatial coordinate r . The notations in the above equations are the same as in [1].

To solve the set of partial differential equations of hyperbolic type with six dependent variables, U_p , U_g , ρ_p , ρ_g , p and T_p , we applied the characteristics method. The families of the characteristic curves may be obtained in general after Sauer's method [4]. One has to solve the determinant $\det |B - \lambda A| = 0$ or

$$\begin{vmatrix} \rho_g & 0 & U_g - \lambda & 0 & 0 & 0 \\ 0 & 0 & 0 & \rho_p & U_p - \lambda & 0 \\ \rho_g (U_g - \lambda) & 1 & 0 & \rho_p (U_p - \lambda) & 0 & 0 \\ \beta_1 & \beta_2 - \alpha_1 \lambda & \alpha_2 (U_g - \lambda) & \beta_3 - \alpha_3 \lambda & 0 & \alpha_4 (U_p - \lambda) \\ 0 & \varepsilon & 0 & \rho_p (U_p - \lambda) & 0 & 0 \\ 0 & 0 & 0 & 0 & 0 & c \rho_p (U_p - \lambda) \end{vmatrix} = 0, \quad (4)$$

where the λ 's associated with each family are the eigenvalues of A . From (4) one may get

$$(U_g - \lambda) (U_p - \lambda)^2 \left[(U_p - \lambda) \{ (U_g - \lambda)^2 - (1 - \varepsilon) a_g^2 \} - \frac{\varepsilon^2}{1 - \varepsilon} \eta \frac{\gamma - 1}{\gamma} a_g^2 (U_g - \lambda) \right] = 0, \quad (5)$$

$$a_g^2 = \gamma \frac{p}{\rho_g}, \quad \text{and} \quad \eta = \frac{\rho_g}{\rho_p},$$

where a_g is the sound speed of the gas and η the loading ratio. Sauerwein and Fendell [5] have already pointed out that the last term in the square brackets of (5) may be negligible. However, one should notice that it is not necessary to put $\varepsilon = 0$, as they have emphasized, since the absolute value of $\varepsilon^2 \eta a_g^2$ is negligible small in comparison with the term of a_g^2 . In this case, one can get the characteristics from (5) by neglecting the last term,

$$\lambda = U_g, \quad \lambda = U_p, \quad \lambda = U_g \pm \sqrt{1 - \varepsilon} a_g, \quad (6)$$

where $\lambda = U_p$ should be counted threefold. The last equation of (6) shows that the sound speed in the mixture is smaller than that in a homogeneous gas by the factor of $\sqrt{1 - \varepsilon}$. If we put $a = \sqrt{1 - \varepsilon} a_g$, the last characteristics in the pseudo-fluid are described by (7).

$$\lambda = U_g \pm a. \quad (7)$$

Thus we can get six characteristics for the system of the six partial differential equations. It is interesting for us to know that in fact the three families of the characteristics $\lambda = U_g$ and $\lambda = U_g \pm a$ may be obtained from the three conservation equations for the gas. It means that the present expressions for the characteristics curves are correct when the interaction between the gas and the particles is negligible. Corresponding to the six characteristic curves, one may get compatibility equations as follows:

along the C_0 characteristic of $dr/dt = U_g$,

$$(1 - \varepsilon) dp - a^2 d\rho_g + [(\gamma - 1) Q + U_m F] dt = 0, \quad (8)$$

along the C_{\pm} characteristics of $dr/dt = U_g \pm a$

$$(1 - \varepsilon) dp \pm a \rho_g dU_g + [(U_m \mp a) F + (\gamma - 1) Q + j \rho_g U_g a^2 / r] dt = 0, \quad (9)$$

along the C_p characteristic

$$dQ_p + Q_p \left(\frac{\partial U_p}{\partial r} - \frac{j}{r} U_p \right) dt = 0, \quad (10)$$

$$\begin{aligned} & b Q_g a_g^2 dU_g - b (U_p - U_g) dp \\ & + [1 + b Q_p \{a_g^2 - (\gamma - 1)(U_p - U_g)^2\}] dU_p \\ & + b (\gamma - 1) Q_p c (U_p - U_g) dT_p \\ & - \left\{ \frac{F}{Q_p} + \frac{j}{r} b a_g^2 Q_g U_g (U_p - U_g)^2 \right\} dt = 0, \end{aligned}$$

$$b = \frac{\varepsilon}{Q_p \{ (1 - \varepsilon \gamma) (U_p - U_g)^2 - a^2 \}}, \quad (11)$$

$$Q_p c dT_p - Q dt = 0. \quad (12)$$

To perform numerical calculations it is necessary to specify explicit forms of the drag force F and the heat transfer Q between the gas and the particles. There are many expressions for them depending on experimental conditions. The drag force may be expressed as in the previous work by

$$F = \frac{\pi}{8} D_p^2 C_D \frac{Q_g}{1 - \varepsilon} (U_g - U_p) |U_g - U_p| n_p, \quad (13)$$

where n_p means the number density of particles and D_p the diameter of the particles. The heat transfer term Q is expressed as

$$Q = \frac{6 \varepsilon \mu}{D_p^2} \frac{c_p N u}{Pr} (T_g - T_p). \quad (14)$$

Equations (13) and (14) are written in simpler form by introducing relaxation times for velocity τ_v and temperature τ_T :

$$\frac{F}{Q_p} = \frac{U_g - U_p}{\tau_v}, \quad \frac{Q}{c Q_p} = \frac{T_g - T_p}{\tau_T} \quad (15)$$

with

$$\tau_v = \frac{m}{3 \pi \mu D_p}, \quad \tau_T = \frac{c m Pr}{c_p 2 \pi \mu D_p}. \quad (16)$$

Boundary Conditions

The foregoing system of characteristic equations are solved under the following boundary conditions: The boundary conditions across the shock discontinuity are given by the generalized Rankine-Hugoniot relation [1]. Frozen conditions across the shock front are used for the particles. Then just behind the shock front, we put

$$U_p = 0, \quad T_p = (T_p)_0 \quad \text{and} \quad Q_p = (Q_p)_0. \quad (17)$$

The conditions across the shock front for the gas are given by

$$\frac{U_g}{a_{g0}} = \frac{2}{\gamma + 1} \left(M - \frac{1}{M} \right) \quad (18)$$

$$\frac{p_g}{p_0} = 1 + \frac{2\gamma}{\gamma + 1} (M^2 - 1) \quad (19)$$

$$\frac{Q_g}{(Q_g)_0} = \frac{(\gamma + 1) M^2}{2 + (\gamma - 1) M^2}, \quad M = \frac{\dot{R}_s}{a_g}, \quad (20)$$

where the subscript zero denotes physical quantities a head of the shock and \dot{R}_s is the shock speed.

Another boundary condition is given near the center of explosion. In a real system there exists a contact surface between the explosives and the surrounding atmosphere. In general, however, it is impossible to determine the motion of the contact surface by using the shock fitting method, since the position of the contact surface should be determined as an eigenvalue at every given time. To remove this difficulty, we considered a generalized piston problem. It is assumed here that the motion of the contact surface may be described as follows:

$$U_c = U_0 \exp(\alpha t), \quad \alpha \leq 0, \quad (21)$$

where U_0 is the initial velocity of the contact surface and α is a parameter. This model is identical to the problem of expanding core. Then the ratio of the core expansion h is introduced to simplify the model and defined as

$$h = \frac{U_c}{\alpha r_0} = \frac{\Delta r_c}{r_0}, \quad (22)$$

where r_0 is the initial position of the core and Δr_c is the displacement of the core corresponding to the time increment Δt . The expansion rate of the core with respect to initial position is denoted by h . Here we have assumed that the core is adiabatic, so that there is no heat exchange through the surface. The present model is a generalization of the piston problem in a shock tube. In this case, we may estimate the explosion energy E as

$$E = \int_{r_0}^r v_j p(r_c, t) r^j dr \quad (23)$$

with

$$v_j = 1, \quad 2\pi, \quad 4\pi \quad \text{for } j = 0, 1, 2.$$

Equation (23) is integrated numerically to estimate the scale of explosions in terms of E .

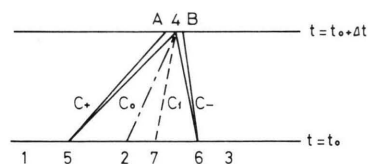
Numerical Calculation

To integrate the basic equations (8) to (12) in the characteristic form numerically, the total derivatives along the characteristics are replaced by the finite difference forms as usual. However, the system of the basic equations does not show the complete form of hyperbolic type, since (10) contains the partial derivative with respect to r . It is very difficult to evaluate the value of this term when the standard technique to integrate the finite difference equations along the characteristics is applied. The Hartree technique [6] overcomes this difficulty, since in applying his technique the grid points are constructed along the constant time lines at every time step. As a result, one can easily evaluate the partial derivative on a constant time line.

In the present analysis, the piston problem was considered in general. Then the analysis was reduced to the two points boundary value problem between the location of the piston and the shock front. To begin the analysis of the finite strength shocks the mesh size of the time increment Δt should be specified. The value of Δt may be determined according to the usual criterion for numerical computations as $(U_g + a) \Delta t < \Delta r$. However, the condition may be replaced by the inequality $\bar{a} \Delta t < \Delta r$ for the problem of blast waves, where \bar{a} is the maximum local sound speed. In fact the flow velocity U_g tends to zero near the center of explosion, whereas the local sound speed increases rapidly. Several computations were performed to determine the spacial mesh size Δr . As a result, we found that the number of grid points had little influence on the accuracy of the computation compared with the allowable error. We decided that it is sufficient for the allowable error of iteration to be less than 0.02. It should be noticed here that the number of grid points is not constant through the computation but increases with time. We were compelled to reduce the grid points, to save computer time, when they became too many. We took 0.005 for the allowable error and 198 for the maximum number of grid points.

The finite solutions are constructed in the (r, t) plane under the above criteria. In the present analysis, it is necessary to know the initial values on the line at a given instant $t = t_0$, when the position and the shock strength are specified on the (r, t) diagram. Here the physical values of 21 points on the

constant time line were evaluated for the gas by making use of Sakurai's series expansion method (7). For the particles the physical values along the initial time line are taken to be constant. These conditions are corresponding to the frozen transition regarding the particles. The solutions along the lines of $t = t_0 + n \Delta t$, $n = 1, 2, \dots, n$, are obtained step by step. To construct the solutions on the constant time line of $t = t_0 + \Delta t$ with the initial condition, we first draw the path line (2, 4) by using the C_0 characteristic line at the point 2. From the point 4 one can inversely construct the C_+ , C_- and C_1 characteristics lines using estimated values of U_g , a and U_p , which intersect the $t = t_0$ line at points 5, 6 and 7. The properties at the point 5, 6 and 7 should be obtained exactly from linear interpolation between those at the points 1, 2 and 3. However, the interpolated values may usually differ from the estimated ones. Then we construct the characteristics lines along C_+ , C_- and C_1 , again using the properties at the points 5, 6 and 7. They may intersect the $t = t_0 + \Delta t$ line at points A and B in the neighbourhood of the point 4. In this case, if the estimated values are sufficiently accurate, the points A and B should coincide at the point 4. This procedure was continued until the required accuracy of the properties at the point 4 was satisfied. Similar processes were adopted for the points on the back boundary and the shock point, where the boundary conditions along the contact surface and also the shock discontinuity in (18) to (19) should be satisfied. In this case, the C_- and C_1 characteristics for the back boundary and the C_+ characteristics for the shock front were taken into account.



Results and Discussion

Generalized piston problems in a dusty gas were studied by the characteristics method. As a typical example, the flow in a shock tube is analysed corresponding to the case $h \rightarrow \infty$. The initial conditions used in this calculation are shown in Table 1. The profiles of the pressure, density, velocity and temperature behind the shock front along the shock

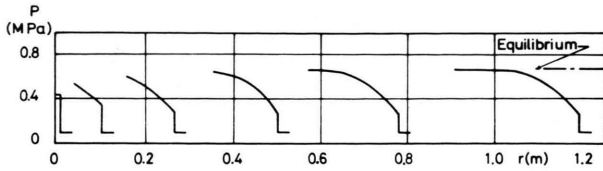


Fig. 1. a) Pressure profiles behind the plane shock wave vs. distance.

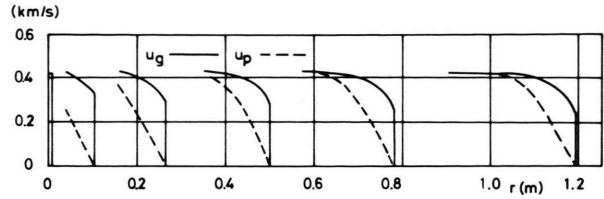


Fig. 1. b) Velocity profiles behind the plane shock wave vs. distance.

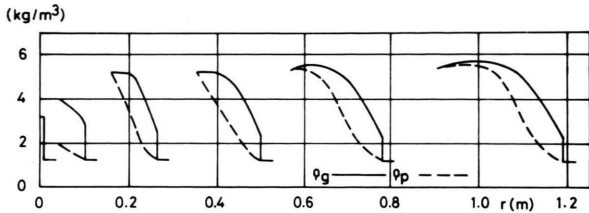


Fig. 1. c) Density profiles behind the plane shock wave vs. distance.

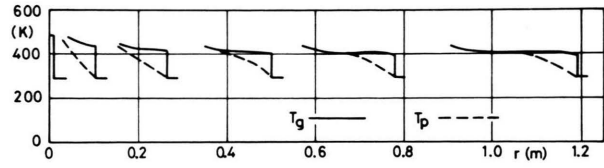


Fig. 1. d) Temperature profiles behind the plane shock wave vs. distance.

tube are shown in Figs. 1(a) to 1(d). Here the solid lines show the change in flow variables of the gas and the dotted lines denote those of the particles along the tube. The starting conditions for the calculation were given by the Rankine-Hugoniot relations for the gas and the frozen condition across the shock wave for the particles. The profiles show that the frozen shock wave of the gas produced in the mixture at first, approaches to the equilibrium shocks. In the early time of shock propagation, the distance between the shock front and the contact surface is small in comparison with the relaxation length so that the equilibrium state is not attained at the contact surface. These relaxation phenomena are strongly affected by the drag law as well as heat transfer between the particles [8]. In this case the particles act as a sink of both momentum and heat energy. It is difficult to compare the present results with the experiments directly, since the profiles show the variation of the physical

properties with distance along the tube, whereas the profiles on a synchroscope show its time history at a given position. However, the discrepancies of the profiles between the gas and the particles are found from the experiments by Frohn, King and Ming [9]. The present analysis shows that the change in physical quantities across the frozen shock front is similar to their experimental results.

The decay of cylindrical blast waves in the dusty gas with different relaxation time are shown in

Table 1. Shock tube flow.

Specific heat ratio of a gas	$\gamma = 1.4$
Relative specific heat ratio of particles	$\delta = 1.0$
Prandtl number	$Pr = 0.73$
Nusselt number	$Nu = 2.0$
Diameter of a particle	$D_p = 7 \times 10^{-6} \text{ m}$
Mass loading ratio	$\eta = 1.0$
Volume fraction of particles	$\varepsilon = 0.001$
Initial Mach number	$M = 2.0$
Core expansion ratio	$h = \infty$
Specific material density ratio	$\zeta = 0.001$

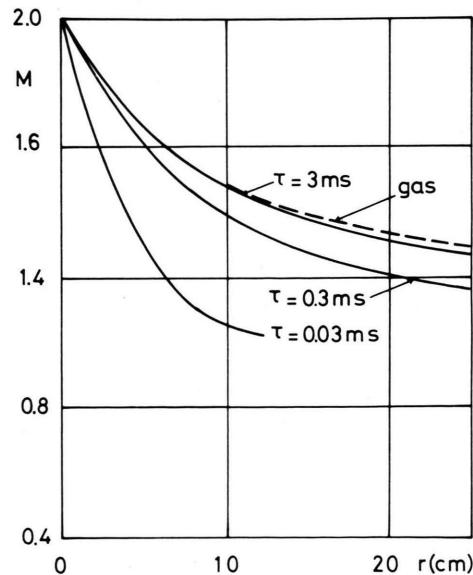
Fig. 2. Decay of the cylindrical blast waves with distance for various relaxation times τ .

Table 2. Blast wave.

Specific heat ratio of a gas	$\gamma = 1.4$
Relative specific heat ratio of particles	$\delta = 1.0$
Prandtl number	$Pr = 0.73$
Nusselt number	$Nu = 2.0$
Diameter of a particle	$D_p = 8 \times 10^{-6} \text{ m}$
Mass loading ratio	$\eta = 1.0$
Volume fraction of particles	$\varepsilon = 0.001$
Initial Mach number	$M = 5.0$
Core expansion ratio	$h = 0.1$
Specific material density ratio	$\zeta = 0.001$

Figure 2. The initial values used in the computation are also shown in Table 2. Here the physical quantities are normalized by the values at the shock front. Here the relaxation times of both velocity and temperature are assumed to be identical and taken as 0.03, 0.3 and 3 ms. For comparison the decay of the blast wave in a pure gas is shown and described by the dotted line in the figure. From the figure we found that the blast wave decayed rapidly for the

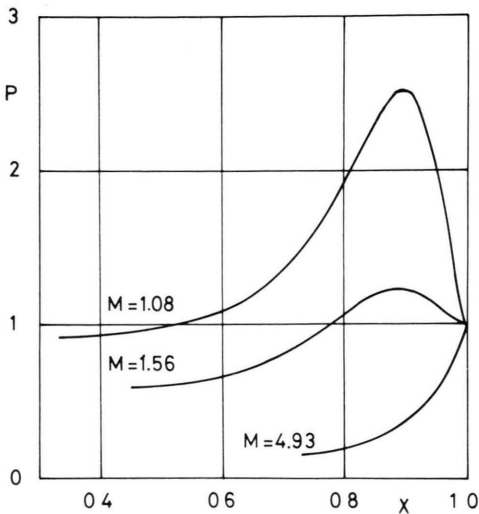


Fig. 3. a) Nondimensional pressure profiles behind the cylindrical blast wave.

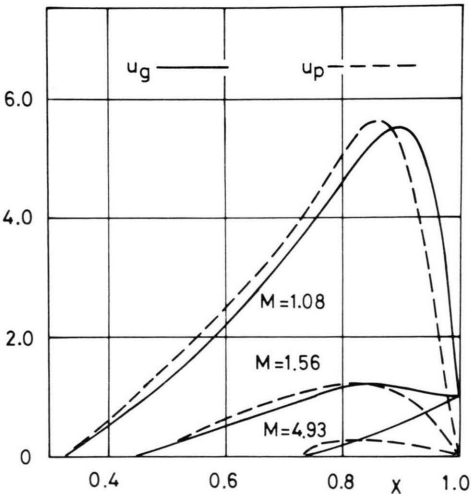


Fig. 3. b) Nondimensional velocity profiles behind the cylindrical blast wave.

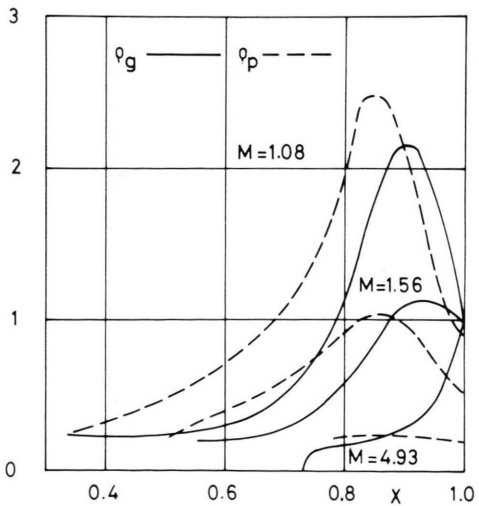


Fig. 3. c) Nondimensional density profiles behind the cylindrical blast wave.

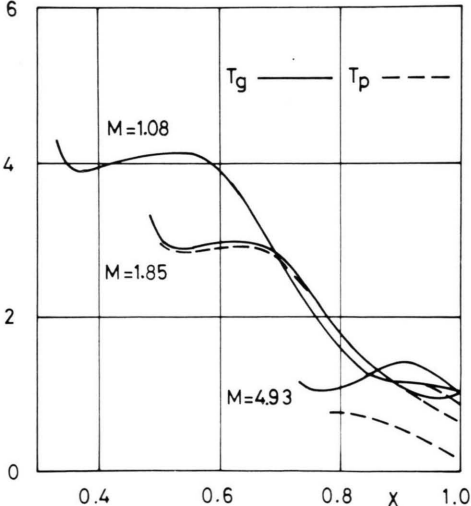


Fig. 3. d) Nondimensional temperature profiles behind the cylindrical blast wave.

Table 3. Notations.

a_g	sound speed of a gas
C_D	drag coefficient; $24/Re$
c	specific heat of a particle
c_p	specific heat of a gas at constant pressure
D_p	diameter of a particle
E	explosion energy
F	internal force between the gas and the particles
Q	heat exchange between the gas and the particles
r	distance from the origine
t	time
h	core expansion ratio
m	mass of a particle
n	number of grid points
n_p	number density of particles
f	form parameter
p	pressure
U_g	velocity of the gas
U_p	velocity of the particles
X	nondimensional distance normalized by the shock radius R_s
Nu	Nusselt number
Pr	Prandtl number
Re	Reynolds number
T_g	gas temperature
T_p	temperature of particles
τ_v	velocity relaxation time
τ_T	temperature relaxation time
γ	specific heat ratio of a gas
δ	relative specific heat ratio of a particle c/c_p
ε	volume fraction of particles
η	mass loading ratio
ρ_g	density of a gas
ρ_p	density of particles
U_0	initial velocity of contact surface

case of small relaxation time. The existence of suspended particles may cause the rapid decay of shock strength. The results may be explained from the fact that the particles can rapidly absorb the energy from the gas in this case. Whereas for the case of large relaxation time the momentum and the heat exchange between the phases are small and the shock wave of the gas may pass through the particle clouds. To clarify the relaxation process of the mixture the results for small relaxation times are shown in Figs. 3(a) to 3(d). In this case the flow is close to the equilibrium flow so that the particles obey the gas flow soon. The profiles of the physical variables behind the shock front in the dusty gas are actually different from the blast wave in pure gas after the elapse of time. The effects of the particles on the profiles are recognized in the near region behind the shock front, where the profiles of the pressure, density and velocity have their maximum values. After the peak the values for both the velocity and the density of the particles exceed

those of the gas. In this region the gas may be accelerated by the particle clouds. Thus the flow field is divided into several regimes which are characterized by the shock position and relaxation time.

As to the energy of explosion E , the present analysis can be compared with the experiments of exploding wires [9]. From (23) the energy used to produce the cylindrical blast wave was estimated to be 3.6 J/cm. On the other hand the energy discharged from the condenser bank into pure gas was about 45 J/cm. Thus 8% of the discharged energy are used for producing the blast wave. This value agrees with the result from the similarity analysis and shows that the present analysis is useful for the analysis on blast waves.

Conclusions

The unsteady flow caused by a piston in a dusty gas was analysed by the method of characteristics. Here Hartree's technique was employed to integrate the characteristics equations numerically. From the results we may conclude as follows:

- 1) The characteristics equations are obtained without neglecting the effect of the partial pressure of the particles.
- 2) The flow in a shock tube as well as the blast wave may be analysed by introduction a generalized piston problem.
- 3) The relaxation processes behind the unsteady shock waves can be explained by the present analysis in general.
- 4) The flow field is divided into several regimes which are characterized by the shock position and the relaxation times.
- 5) It is confirmed that the existence of suspended particles may cause the rapid decay of shock strength.

Acknowledgements

The author would like to express his appreciation to Prof. H. Grönig, RWTH Aachen, for helpful discussions and interest. He is also indebted to Mr. Klose and Mrs. von Hoegen for considerable assistance in preparation and to Mr. K. Ishikura for the numerical computation.

The author also wishes to thank the Alexander von Humboldt-Stiftung.

- [1] F. Higashino and T. Suzuki, *Z. Naturforsch.* **35 a**, 1330 (1980).
- [2] T. Suzuki, F. Higashino, and A. Takano, *Proc. 10th Int. Shock Tube Symp.*, 158 (1975).
- [3] G. Rudinger and A. Chang, *Phys. Fluids* **7**, 1747 (1964).
- [4] R. Sauer, *Nichtstationäre Probleme der Gasdynamik*, Springer-Verlag, Berlin 1966, p. 58.
- [5] H. Sauerwein and F. F. Fendell, *Phys. Fluids* **8**, 1564 (1965).
- [6] P. C. Chou and S. L. Huang, *J. Appl. Phys.* **40**, 752 (1969).
- [7] A. Sakurai, *Blast Wave Theory, Development in Fluid Dynamics I*, Academic Press, New York 1965, p. 309.
- [8] K. Ishikura, Master thesis, Tokyo-Noko University 1977.
- [9] A. Frohn, G. König, and J. Ming, *Neue Wege in der Mechanik*, VDI, Düsseldorf, Festschrift zum 75. Geburtstag von Prof. Schultz-Grunow; *Inst. Allg. Mech.*, RWTH Aachen 1981, p.79.